

# Ferroelectric and Ferroelastic Domain Wall Motion in Unconstrained $\text{Pb}(\text{Zr},\text{Ti})\text{O}_3$ Microtubes and Thin Films

Srowthi S. N. Bharadwaja, *Member, IEEE*, Paul J. Moses, Susan Trolier-McKinstry, *Fellow, IEEE*, Theresa S. Mayer, Paolo Bettotti, and Lorenzo Pavesi

**Abstract**—Ferroelectric polarization switching of high aspect ratio ( $>80:1$ )  $\text{PbZr}_{0.52}\text{Ti}_{0.48}\text{O}_3$  (PZT) microtubes with a wall thickness of  $\sim 200$  nm was investigated. A charge-based technique was used to assess the dielectric and ferroelectric properties of individual mechanically-unconstrained PZT microtubes with interdigitated electrodes. An enhancement in the degree of ferroelastic (non- $180^\circ$ ) domain wall motion was observed in the tubes relative to films of similar thickness on rigid substrates. The dielectric response of the tubes showed a Rayleigh-like ac field dependence over a wide temperature range; the extent of the extrinsic contribution to the dielectric response dropped as the temperature approached 10K, but remained finite. This work demonstrates a general methodology for directly electrically addressing small, unconstrained ferroelectric devices, extending the range of driving fields and temperatures over which these materials can be probed.

## I. INTRODUCTION

FERROELECTRICITY scales extremely well, so that coherent epitaxial films retain ferroelectricity down to only a few unit cells in thickness [1]–[3]. However, most ferroelectric thin films are under hundreds of MPa to GPa of in-plane stress [4], [5]. These stresses can shift the transition temperature [6], alter the equilibrium domain structure [7], change the order of the phase transition, affect the domain wall mobility, and shift the phase transition sequence as a function of temperature [8]. An understanding of the mechanical boundary conditions that control the property scaling in terms of ferroelectric and ferroelastic domain switching is essential to nonvolatile memories, capacitors, piezoelectric microelectromechanical systems (MEMS), and tunable photonic devices [9], [10]. Thus, it is interesting to compare the properties of fully mechanically clamped films on rigid substrates with unclamped structures.

Manuscript received September 21, 2009; accepted December 28, 2009. This work was supported by the Penn State Materials Research Institute, the Commonwealth of Pennsylvania, and by NSF through the Material Research Science and Engineering Center Program (DMR-0080019 and DMR-0213623). The devices were fabricated at the PSU site of the NSF NNIN under grant #0335765.

S. S. N. Bharadwaja, P. J. Moses, and S. Trolier-McKinstry are with the Materials Research Institute, The Pennsylvania State University, University Park, PA (e-mail: bss11@psu.edu).

T. S. Mayer is with the Electrical Engineering Department, The Pennsylvania State University, University Park, PA.

P. Bettotti and L. Pavesi are with the Physics Department, University of Trento, Povo, Italy.

Digital Object Identifier 10.1109/TUFFC.2010.1483

Several methods have been reported to process unconstrained ferroelectric islands, including e-beam patterning [11], focused ion beam writing [12], ferroelectric nanoparticle growth [13], deposition by self organization [14], [15], and template based methods [16], [17]. The majority of the existing studies on ferroelectric nano-structured islands were based either on structural or piezoelectric force microscopy probes [18], [19], with limited high-resolution capacitance measurements on finely patterned epitaxial films [20]. However, missing from the literature is *direct* electrical evidence of ferroelectric switching in these structures as well as a general methodology that allows the electrical properties of ferroelectricity in individual microtubes to be assessed. Direct polarization switching measurements on ferroelectric microtubes with submicrometer wall thickness could eliminate large potential artifacts, including Maxwell stresses that mimic a piezoelectric response in poled porous insulators or topology-induced errors in nanowire piezoforce microscopy measurements [21].

In this work, a mold replication technique that provides good control of the thickness and composition of the ferroelectric layers was employed [16]. Unconstrained, high aspect ratio (80:1) perovskite PZT microtubes with submicrometer wall thicknesses were prepared in silicon templates using a liquid source misted chemical deposition (LSMCD) technique as described by Morrison *et al.* [22]. A charge-based method was used to assess the dielectric and ferroelectric properties of individual PZT microtubes with interdigitated electrodes. In this paper, it is shown that poling of the microtubes induces more non- $180^\circ$  (ferroelastic) domain wall motion than is observed in PZT films on rigid substrates. In addition, the ac field dependence of the domain wall contributions to the dielectric response is described using the Rayleigh formalism under sub-switching conditions [23], [24].

## II. EXPERIMENTAL PROCEDURE

### A. Fabrication of High Aspect Ratio PZT Microtube Structures

High aspect ratio PZT microstructures were deposited onto the sidewalls of patterned silicon templates using a 1.1M, lead zirconate titanate (PZT) metal-organic decomposition precursor (Ferro Technology Co., Higashi-Matsuyama City, Japan) via LSMCD (Fig. 1). In the LSMCD

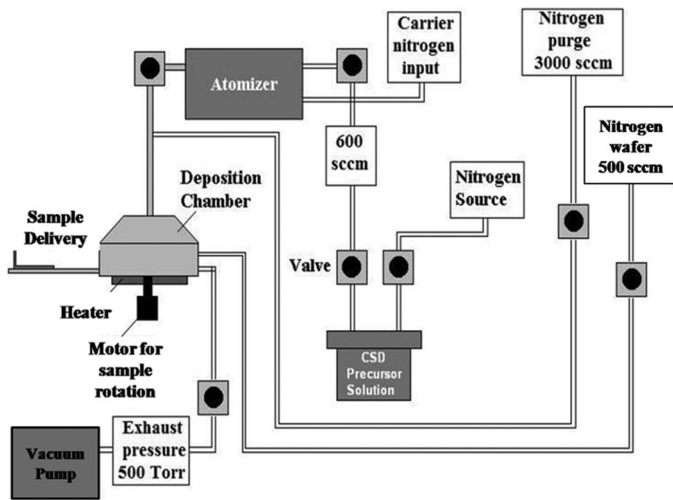


Fig. 1. Schematic of liquid source misted chemical deposition system.

technique, the precursor is nebulized into fine mist droplets under pressurized nitrogen gas using an atomizer. These mist particles are carried through a showerhead using the nitrogen carrier gas. Inside the deposition chamber, the mist droplets are charged and accelerated with a large electric potential (8 kV) toward an electrically grounded wafer. Silicon templates prepared using anodic etching and having  $\leq 1 \mu\text{m}$  diameter pore channels with aspect ratios of  $> 80:1$  were employed to fabricate high aspect ratio PZT submicrometer diameter structures [25]. The pore channels of the silicon templates were pre-cleaned using an anhydrous HF (AHF)/methanol mixture in a mist-based etching module followed by a UV/ $\text{Cl}_2$  exposure to remove residual fluorine from the Si surface.<sup>1</sup> During PZT deposition, the chamber pressure was maintained at 500 mTorr for 5- to 6-min long PZT depositions; the silicon templates were maintained at 40 to 50°C. The top surface of the templates was cleaned with 2-methoxyethanol after each deposition and the wafer was subsequently pyrolyzed at 275°C for 2 min. This process was repeated several times to build up the PZT layer in the templates to the desired wall thickness ( $\sim 200 \text{ nm}$ ). As reported previously, chemical reactions between the lead in the PZT tubes and the surrounding Si mold produce secondary phases during high temperature crystallization [16]. Therefore, after the final deposition, a brief  $\text{CF}_4:\text{O}_2$  plasma etch was used to remove any residual gel as well as the native  $\text{SiO}_2$  layer from the top of the Si templates. A  $\text{XeF}_2$  etch operated at a pressure of 1 Torr with a pulse cycle of 1 min was used to partially release the tubes (Xetch e' series, Xactix Inc., Pittsburgh, PA). In most cases, 60 to 70  $\mu\text{m}$  of Si was removed to produce free-standing PZT microtubes anchored at the bottom. These microtubes were crystallized at 750°C for 2 to 3 min in 99.98% oxygen using a rapid thermal annealer. Subsequently, these tubes were released from the substrate by rinsing in isopropanol.

<sup>1</sup>This step is performed to remove the native  $\text{SiO}_2$  before putting PZT layers on the sidewalls of the silicon. This allowed us to prepare PZT microtubes without  $\text{SiO}_2$  remaining on the surface.

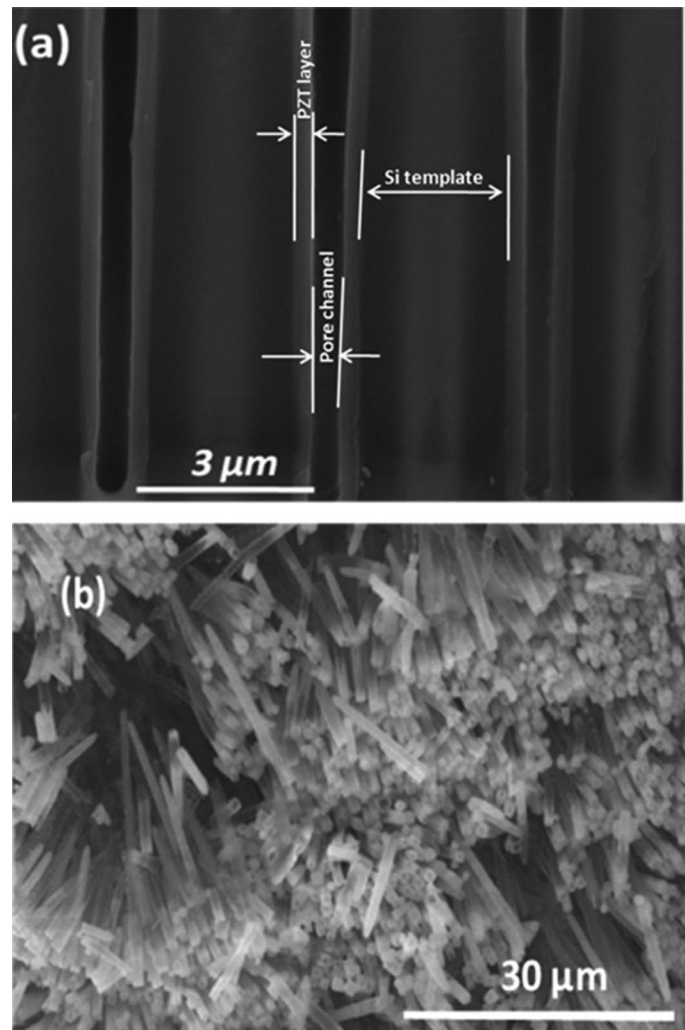


Fig. 2. Scanning electron microscope images of (a) PZT layers at the bottom of the template before release and (b) the released and crystallized PZT tubes with  $>80:1$  aspect ratios.

### B. Structural Characterization

A scanning electron microscope image of the released crystalline tubes is shown in Fig. 2. The synthesized PZT microtubes have a wall thickness of  $\sim 200 \text{ nm}$  and extend to over 80  $\mu\text{m}$  in length. It was shown previously that tubes processed using similar heating profiles have grain sizes of  $\sim 100$  to 150 nm [16]. Structural characterization on the tubes was carried out via X-ray diffraction (Scintag) using  $\text{CuK}\alpha$  radiation over a  $2\theta$  range from 20° to 65° with a 0.025° step size and a 1 s count time/step. X-ray diffraction patterns of an array of tubes show polycrystalline perovskite phase peaks in addition to the presence of an oxyfluoride phase, which probably develops during the  $\text{XeF}_2$  etch [16].

To assess the development of the fluoride phase associated with the  $\text{XeF}_2$  etch, planar PZT thin films were deposited on Pt-coated silicon substrates using the same chemical precursor. Exposing amorphous PZT thin films (after pyrolysis) to a  $\text{XeF}_2$  release etch followed by crystallization at 750°C for 2 min confirmed the formation of the

second phase peak. A mild boric acid can dissolve many fluorides [26] and hence, the PZT films were exposed to 0.1 M boric acid for 2 min after the  $\text{XeF}_2$  treatment to minimize the second phase. Subsequently these films were crystallized in the rapid thermal annealer in oxygen. X-ray analysis confirms pure perovskite phase [Fig. 3(a)]. The dielectric constant and loss tangent of the resultant films (boric acid treated) are 980 and 4.5% respectively, and the dc voltage dependent dielectric data are comparable to PZT thin films (dielectric constant = 980 and loss = 3.7%) that are never exposed to  $\text{XeF}_2$  and boric acid as shown in Fig. 3(b) and (c). This suggests that the boric acid treatment following  $\text{XeF}_2$  etch does not degrade the dielectric properties of the films appreciably. Thus, in this work the presence of fluoride second phase on PZT microtubes was minimized by mild boric acid treatment.

### C. Interdigitated (IDT) Electrode Integration onto Single PZT Tube

A schematic process flow of single PZT tube integration for electrical characterization is shown in Fig. 4. The PZT microtubes were electrically characterized using an IDT electrode capacitor structure, as shown in Fig. 5(a). Fully-released crystallized microtubes were randomly dispersed from an isopropanol solution onto a  $p^+$ -silicon substrate ( $\rho \sim 0.001 \Omega\text{-cm}$ ) covered with 500 nm of thermally grown  $\text{SiO}_2$ . The electrodes (with fingers 4  $\mu\text{m}$  wide, 2  $\mu\text{m}$  spacing) and a surrounding shielding layer were defined by optical lithography followed by liftoff of a 100-nm-thick sputtered Pt film. The surfaces of the microtubes were treated with boric acid before depositing the Pt electrodes and also after the liftoff to minimize the oxyfluoride phase contamination. To improve the electrical interface between the electrodes and the PZT microtube, the structures were annealed at 550°C for 5 min. A schematic and an SEM image of a fully-integrated IDT microtube structure are shown in Fig. 5(b). The capacitance versus dc voltage and small signal dielectric properties were measured as a function of temperature using a cryogenic probe station (model TTP6, LakeShore Cryotronics, Inc., Westerville, OH) in conjunction with a temperature controller (model 332, LakeShore Cryotronics, Inc.).

## III. RESULTS AND DISCUSSION

It is critical in measuring small dielectric structures ( $\sim$ femtofarad) to minimize the effect of stray capacitances (that can be much greater than that of the device) [20], reduce the effect of conduction from leaky dielectrics or surfaces [27], and achieve the signal-to-noise ratio necessary for attofarad resolution. To accomplish this, measurements of the IDT PZT microtube structures were done with a charge-to-voltage converter (1 V/nC) and a lock-in amplifier (model 730, Stanford Research Systems Inc., Sunnyvale, CA) combination with a 10 attofarad resolution capability. A schematic of the electrical circuit is

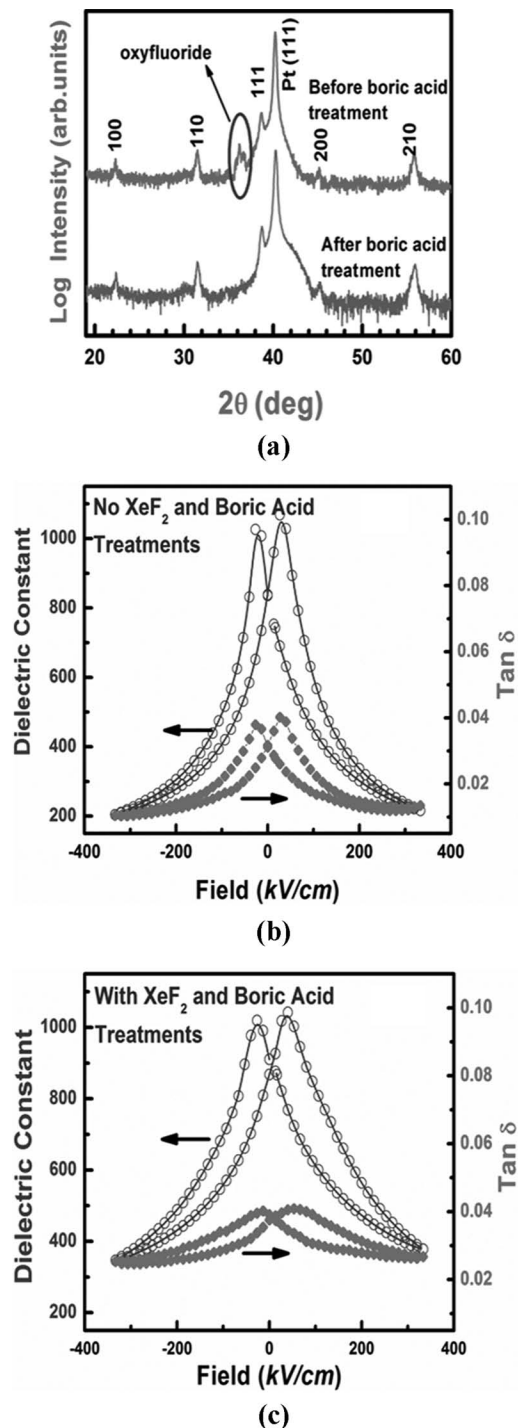


Fig. 3. (a) X-ray diffraction patterns of PZT thin films annealed without and with boric acid treatment after the  $\text{XeF}_2$  etching step. Capacitance and tangent loss values as a function of dc bias in annealed PZT films (b) not exposed to  $\text{XeF}_2$  and boric acid treatments and (c)  $\text{XeF}_2$ -exposed followed by boric acid treatment.

shown in Fig. 5(c). The shield layer deposited over the free surface of the sample served to reduce stray capacitances caused by fringing field effects. To reduce stray capacitance between the shielded probe tips, the contact pads were spaced widely. To minimize fringing through the substrate, heavily doped Si was employed. The substrate was fixed to the copper surface of a printed circuit board using

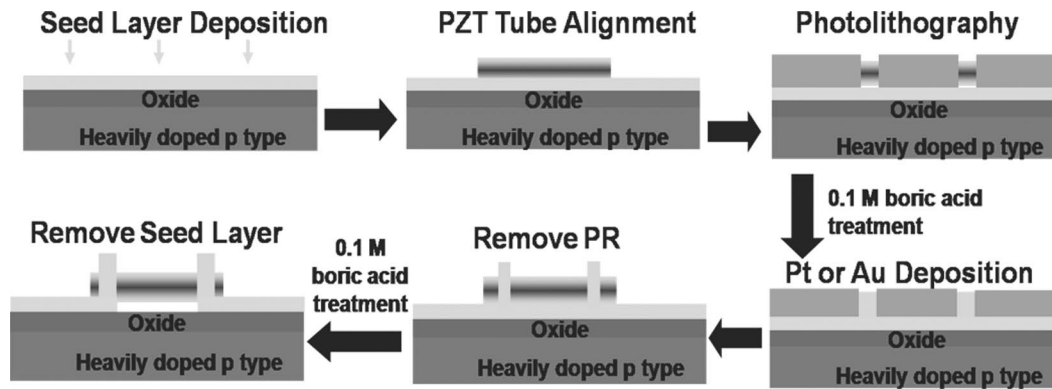


Fig. 4. Schematic steps of PZT tube integration with interdigitated electrodes. PR means photoresist.

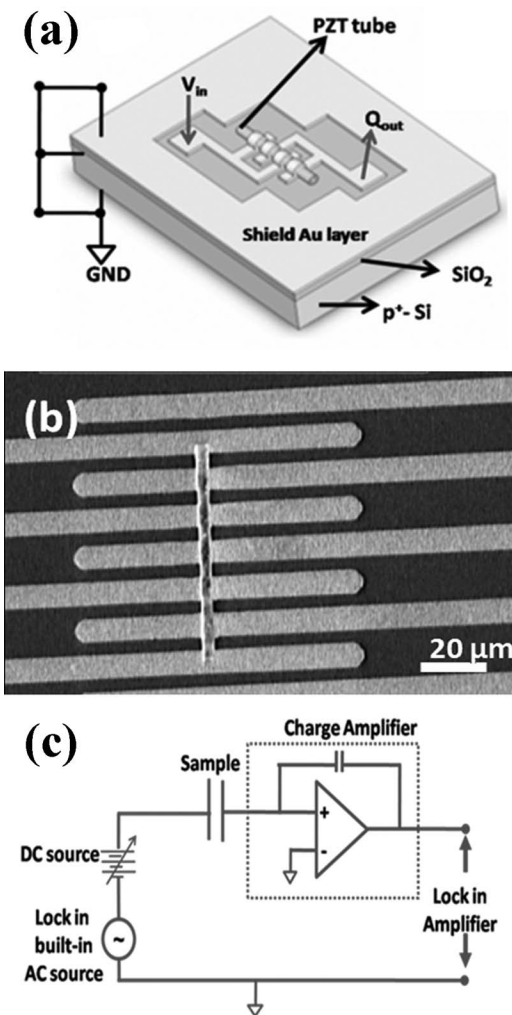


Fig. 5. (a) Schematic of electrical test bed structure, (b) scanning electron microscope image of integrated PZT microtube, and (c) electric circuit model for low capacitance measurements.  $V$  is voltage, and  $Q$  is charge.

conductive epoxy; the circuit board was connected to the system shield, effectively turning the entire substrate into an electrical shield [Figs. 5(a) to 5(c)].

To quantify the stray capacitance and leakage effects, IDT electrodes of the same geometry on the same substrate, but without a PZT tube, were analyzed as a func-

tion of both ac field amplitude and dc bias voltage (with a superimposed  $1 V_{\text{rms}}$  ac signal) between 10 Hz and 10 kHz over a temperature range of 10 to 300K, as shown in the inset of Fig. 6. The capacitance of the bottom thermal oxide layer measured with IDT electrodes was found to be constant with ac voltage and temperature variations as shown in Figs. 6(a) and 6(b), respectively. The estimated temperature coefficient of the stray capacitance was  $\sim(1.2 \pm 0.1) \times 10^{-5} K^{-1}$ , which is close to the reference value for  $\text{SiO}_2$   $2.44 \times 10^{-5} K^{-1}$  [28], [29]. The stray capacitance is primarily a result of two dielectric media, the thermally grown  $\text{SiO}_2$  and the surrounding air between the IDT electrodes. A constant capacitance value of  $\sim 2.84$  fF was measured for the empty IDT between  $-60$  to  $+60$  V dc bias voltages superimposed with a  $1 V_{\text{rms}}$  ac signal [inset of Fig. 6(c)]. On the other hand, individual PZT microtubes with IDT electrodes exhibited a clear butterfly behavior in the capacitance-voltage response measured at 1 kHz, as shown in Fig. 6(c). The measured loss tangents were less than 5% over a wide temperature and field range. The observed hysteresis is direct confirmation of ferroelectricity in the PZT microtubes. After subtracting the stray capacitance, the zero bias capacitance of the PZT tube is  $\sim 5.75$  fF at 1 kHz. To the authors' knowledge, these are the first direct *electrical* measurements of ferroelectric behavior in such PZT microtubes.

It is well known that the functional properties in ferroelectrics are influenced by the mechanical boundary conditions. In bulk PZT ceramics, domain wall motion contributes  $\sim 30$  to  $50\%$  of the dielectric and piezoelectric properties at room temperature [30], [31]. On the other hand, the extrinsic contribution to the piezoelectric response in ferroelectric thin films is heavily limited, in part, because of clamping of non- $180^\circ$  domain wall motion by the substrate. To examine the domain wall motion in the PZT microtubes that are largely decoupled mechanically from the substrate, the dielectric response was investigated under sub-switching field conditions and described using Rayleigh analysis. In the Rayleigh approach, when an oscillating field with an amplitude  $E_o$  ( $\ll E_c$ , coercive field) is applied, the resultant polarization,  $P(E)$ , and dielectric permittivity,  $\epsilon$ , can be described as [32], [33]:

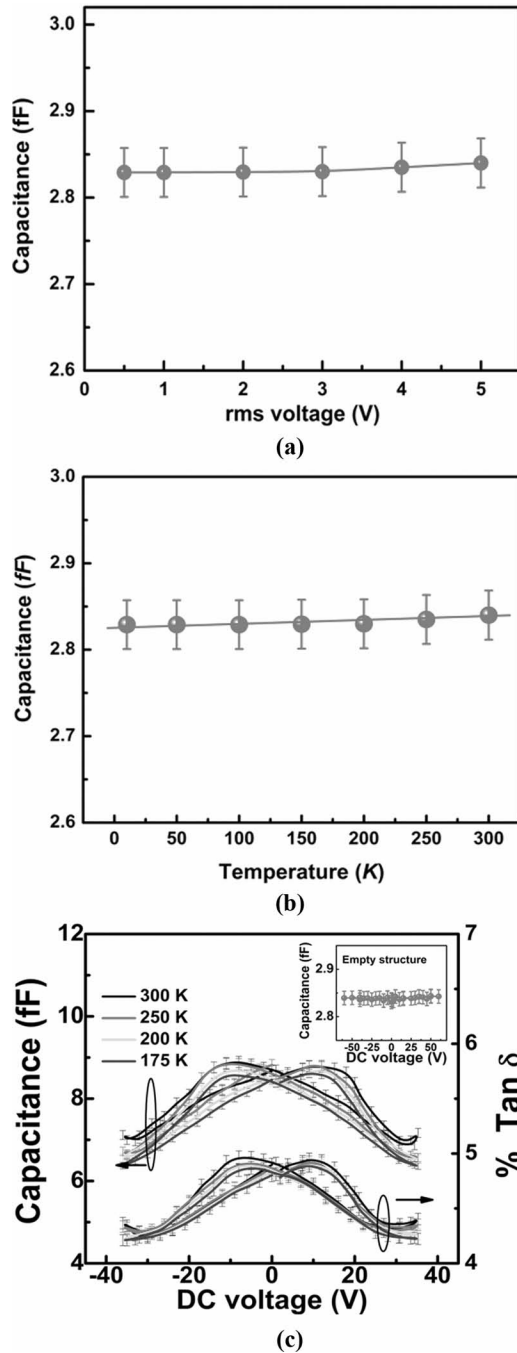


Fig. 6. Capacitance of an empty IDT structure as a function of (a) excitation electrical signal  $V_{\text{rms}}$ , (b) temperature at 1 kHz with a 1  $V_{\text{rms}}$  oscillation level, and (c) capacitance and loss tangent of a PZT tube as a function of dc bias. The inset in (c) represents the variation of capacitance with dc bias of an empty IDT structure.

$$P(E) = (\varepsilon_{\text{init}} + \alpha E_o)E \mp \frac{\alpha}{2}(E_o^2 - E^2) \quad (1)$$

$$\varepsilon(E) = \frac{\partial P}{\partial E} = \varepsilon_{\text{init}} + \alpha \cdot E, \quad (2)$$

where  $E$  ( $= E_o \cdot \sin\omega t$ ) is the applied ac field,  $\varepsilon_{\text{init}}$  is the initial dielectric permittivity (the sum of the intrinsic lattice response and reversible domain wall contribu-

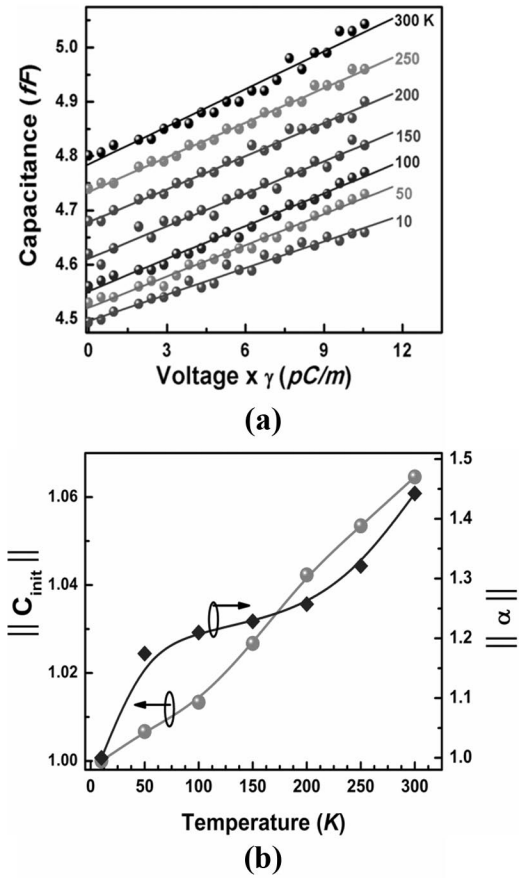


Fig. 7. (a) AC field dependence of the capacitance on a PZT microtube structure as a function of temperature, and (b) normalized Rayleigh parameters.

tions), and  $\alpha$  represents the irreversible contribution due to domain wall motion. Validation of Rayleigh behavior in a PZT microtube between interdigitated electrode structures was carried out in terms of measured capacitance,  $C$ , as a function of excitation voltage ( $V_{\text{ac}}$ ).

$$C = C_{\text{init}} + \alpha(\gamma \cdot V_{\text{ac}}), \quad (3)$$

where  $C_{\text{init}}$  is the initial capacitance,  $V_{\text{ac}}$  is the ac excitation voltage, and  $\gamma$  is the geometrical factor (in farads per meter) of the capacitor structure. For an IDT capacitor associated with  $n$  gaps and thin film capacitor structure,  $\gamma$  can be expressed as

$$\gamma = \frac{n \cdot \varepsilon_o \cdot (\text{Area of capacitor})}{(\text{Electrode spacing})^2} \quad (4)$$

$$\gamma = \frac{\varepsilon_o \cdot (\text{Area of capacitor})}{(\text{Film thickness})^2}. \quad (5)$$

The scaling factor  $\gamma$  is used for normalizing geometries in estimating the electric field distributions and to compare the electrical measurement results of tubes with those of thin films. Following (3), the response of a PZT microtube capacitance versus scaled voltage ( $\gamma \cdot V_{\text{ac}}$ ) over a temperature range of 10 to 300K is shown in Fig. 7. As can be seen

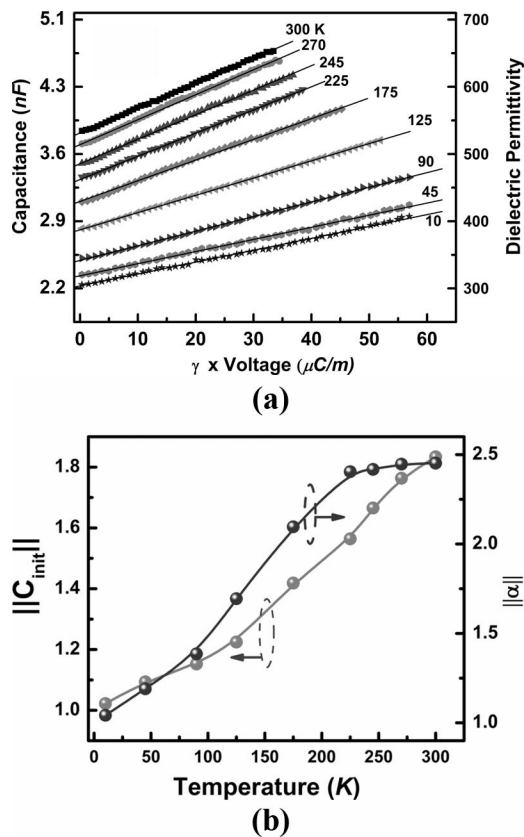


Fig. 8. (a) AC field dependence of the capacitance for a 220-nm-thick PZT film as a function of temperature, and (b) normalized Rayleigh parameters.  $\gamma$  for the PZT film is  $1 \times 10^{-6}$  F/m.

from Fig. 7(a), the linear dependence of the capacitance on the voltage confirms Rayleigh-like behavior in the unconstrained PZT microtube down to 10K.

As temperature is reduced, the domain wall contributions to the dielectric response decrease [30], [34]. As a result, the ratio of the reversible to irreversible Rayleigh parameters increases compared with the room temperature value [35], [36]. As shown in Fig. 7(b), in the unconstrained PZT microtubes, the normalized irreversible Rayleigh parameter  $\|\alpha\|$  is  $\sim 40$  to  $45\%$  higher at 300K relative to 10K. In contrast, normalized  $C_{\text{init}}$ , (intrinsic lattice + reversible domain wall motion) is decreased only  $\sim 6$  to  $7\%$  at 10K compared with 300K. Although domain wall motion decreases as temperatures approach 0K, it is worth noting that at 10K, the observation of a nonzero  $\alpha$  value for the PZT tubes suggests that domain walls can still be excited at larger ac electric fields [37].

A similar analysis was conducted on  $\text{Pb}(\text{Zr}_{0.52}\text{Ti}_{0.48})\text{O}_3$  thin films prepared from the same solution chemistry using comparable processing conditions on rigid Pt-coated Si substrates [32], see Fig. 8. The  $\epsilon_{\text{init}}$  (or  $C_{\text{init}}$ ) at  $E_{\text{ac}} = 0$  decreased from 540 ( $\sim 3.9$  nF) to 320 ( $\sim 2.2$  nF) as the temperature decreased from 300K to 10K. Thus, the room temperature  $\epsilon_{\text{init}}$  (or  $C_{\text{init}}$ ) is approximately 70% larger than the value at 10K and exhibited an increase of  $\sim 250\%$  in  $\|\alpha\|$  between 10 and 300K.

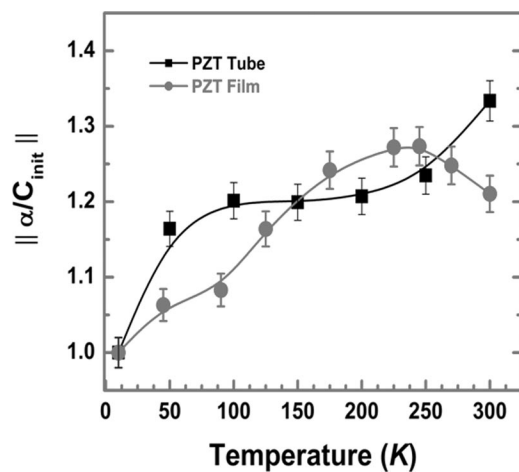


Fig. 9. Normalized irreversible to reversible Rayleigh parameters in PZT thin film ( $\sim 220$  nm) and PZT microtubes.

It has been reported that the intrinsic dielectric constant in PZT (52/48) ceramics is  $\sim 350$  to  $400$  and undergoes a drop of  $\sim 10\%$  from 300K to 0K [38]–[41]. The larger temperature dependence for the permittivity of the film is attributed to the progressive reduction in domain wall contributions to the total permittivity, as has been described elsewhere [4], [31], [38]. The relatively small temperature dependence of the initial parameters of the PZT microtube (below that of the intrinsic temperature dependence for PZT), suggests 1) existence of defects in the PZT microtube or an interfacial layer between the electrodes and PZT (even with mild boric acid rinsing); 2) differences in the electric field distribution in the cases of the PZT microtube with IDT electrodes and the metal-PZT-metal thin film configuration. Either of these factors influences the field distribution across the thickness of PZT microtube and can also decrease the irreversible Rayleigh parameter and its temperature dependence.

The temperature dependence of the ratio of the Rayleigh parameters was also examined to evaluate irreversible to reversible domain wall contributions in PZT microtube and thin film structures, as shown in the Fig. 9. It was found that the normalized  $(\alpha/C_{\text{init}})$  value for the microtube increased by  $\sim 35\%$ , compared with the PZT thin film (20 to 28% change) over the temperature range from 10 to 300K. At least three factors complicate the interpretation of the temperature dependence of  $\alpha/C_{\text{init}}$ . First, the dielectric thickness between electrodes is different for the tubes and the films ( $\sim 2000$  versus  $220$  nm), and there is a finite thickness dependence of the permittivity and non-linearity in constrained films [34]. Second, the existence of structural imperfections and/or field distributions will necessarily introduce artifacts in the temperature dependence of the Rayleigh parameters of the tube (relative to the temperature dependence of the PZT making up the tube). As a result, no strong conclusions can be drawn as to the relative mobility of domain walls in the tubes versus films based on this data set. Third, differences in grain size may also contribute [42].

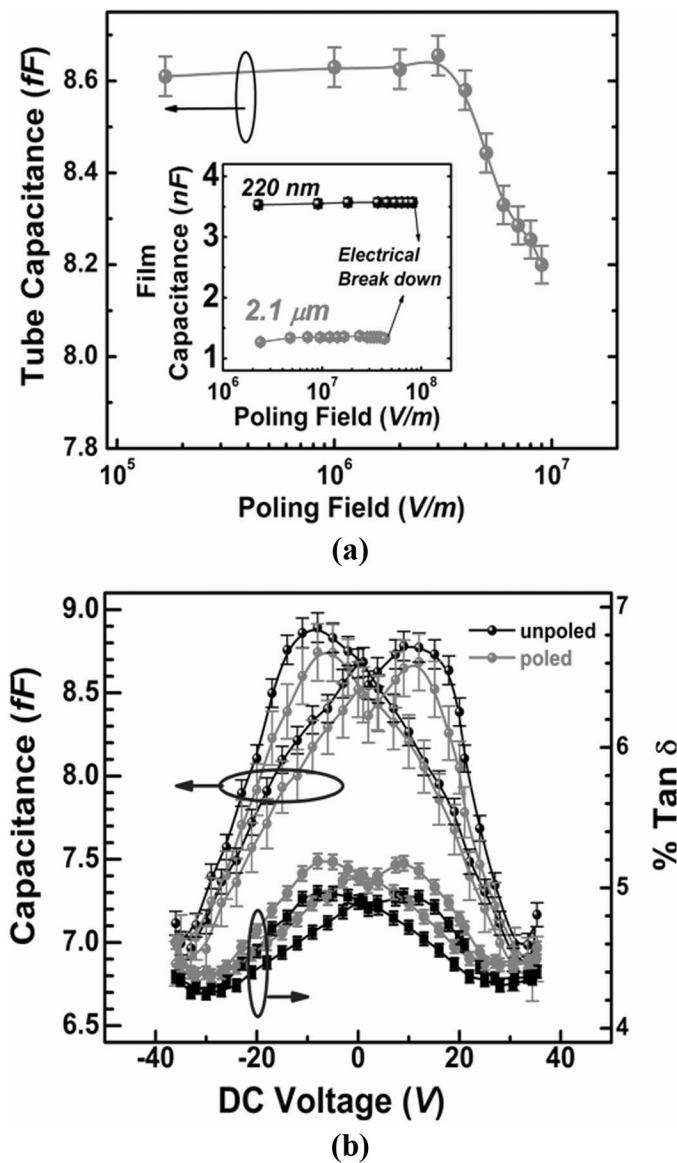


Fig. 10. (a) Capacitance as a function of poling field in PZT free standing tube and clamped thin films. The wall thickness of the PZT tube is  $\sim 220$  nm. (b) PZT tube capacitance as a function of dc bias before and after poling with a 10 MV/m field.

To provide additional insight, the room temperature capacitance was examined after poling a microtube. The data were compared with those for 220-nm-thick (i.e., approximately the PZT tube's wall thickness) and 2- $\mu$ m-thick (i.e., approximately the spacing between the IDT electrodes) PZT films on Pt-coated  $\text{SiO}_2/\text{Si}$  substrates. In all cases, samples were poled for 10 min at room temperature at various dc bias fields. Fig. 10(a) compares the capacitance values measured at 1 kHz with a 1 V<sub>rms</sub> oscillation voltage as a function of the poling field. In the PZT thin films, increased poling field strength has little effect on the measured capacitance until electrical breakdown, suggesting that non-180° domain switching is strongly clamped in the PZT films [4]. In contrast, the capacitance of a PZT tube decreased by  $\sim 6\%$  upon poling, indicating a change in the low-field dielectric response in the poled microtubes. To confirm that the decrease in the capacitance

of PZT microtube is caused by domain switching and is not an artifact associated with electrode delaminations or sample degradation etc., the ferroelectric hysteresis was measured again after poling at 10 MV/m for 10 min. Fig. 10(b) shows the hysteresis measurements on a PZT microtube before and after poling. The resultant data was found to fall within experimental error of the unpoled value, suggesting that the drop in the capacitance upon poling [Fig. 10(a)] was indeed caused by the ferroelastic domain state change in the microtube. That is, most perovskites have smaller dielectric constants parallel to the polarization axis than perpendicular to it. Ferroelastic switching thus decreased the permittivity at low fields on poling. These measurements indicate that the degree of non-180° domain wall motion is substantially larger in the tubes than the films. It is likely that this difference stems, at least in part, from the release of the stresses and mechanical constraints imposed by the substrate. Differences in grain size may also contribute.

#### IV. SUMMARY

In summary, ferroelectric polarization switching of unconstrained PZT microtubes having capacitance values of  $\sim 5$  fF was characterized using a charge measurement technique. It was found that non-180° domain switching in the continuous films is heavily restricted, presumably, at least in part, because of mechanical clamping from the substrate. However, non-180° domain reorientation is possible in unconstrained PZT microtubes having 220 nm thick walls. It is also possible that a difference in grain size may have contributed to the observed disparity between the tubes and the films. The general methodology outlined in this paper allows the functional properties of ferroelectric materials to be probed to even smaller wall thicknesses. This, in turn, will facilitate understanding of the effect of mechanical boundary conditions on the scaling of the dielectric properties.

#### ACKNOWLEDGMENTS

The authors are thankful to Dr. P. Bintachitt (PSU) for providing PZT films and Dr. P. Roman (Primaxx Inc., Allentown, PA) for assisting in use of the LSMCD etch system.

#### REFERENCES

- [1] D. D. Fong, G. B. Stephenson, S. K. Streiffer, J. A. Eastman, O. Auciello, P. H. Fuoss, and C. Thompson, "Ferroelectricity in ultrathin perovskite films," *Science*, vol. 304, no. 5677, pp. 1650–1653, 2004.
- [2] V. Nagarajan, J. Junquera, J. Q. He, C. L. Jia, R. Waser, K. Lee, Y. K. Kim, S. Baik, T. Zhao, R. Ramesh, Ph. Ghosez, and K. M. Rabe, "Scaling of structure and electrical properties in ultrathin epitaxial ferroelectric heterostructures," *J. Appl. Phys.*, vol. 100, art. no. 051609, Sep. 2006.
- [3] T. Tybell, C. H. Ahn, and J.-M. Triscone, "Ferroelectricity in thin perovskite films," *Appl. Phys. Lett.*, vol. 75, pp. 856–858, Aug. 1999.
- [4] F. Xu, S. Trolier-McKinstry, W. Ren, B. M. Xu, Z. L. Xie, and K. L. Hemker, "Domain wall motion and its contribution to the dielectric

- and piezoelectric properties of lead zirconate titanate thin films," *J. Appl. Phys.*, vol. 89, pp. 1336–1348, Jan. 2001.
- [5] B. A. Tuttle, J. A. Voigt, T. J. Garino, D. C. Goodnow, R. W. Schwartz, D. L. Lippa, T. J. Headley, and M. O. Eatough, "Chemically prepared  $\text{Pb}(\text{Zr},\text{Ti})\text{O}_3$  thin films: The effects of orientation and stress," in *Proc. Eighth IEEE Int. Symp. Applications of Ferroelectrics*, 1992, pp. 344–348.
- [6] G. A. Rossetti, L. E. Cross, and K. Kushida, "Stress-induced shift of the Curie-point in epitaxial  $\text{PbTiO}_3$  thin-films," *Appl. Phys. Lett.*, vol. 59, pp. 2524–2526, Nov. 1991.
- [7] S. K. Streiffer, C. B. Parker, A. E. Romanov, M. J. Lefevre, L. Zhao, J. S. Speck, W. Pompe, C. M. Foster, and G. R. Bai, "Domain patterns in epitaxial rhombohedral ferroelectric films. I. Geometry and experiments," *J. Appl. Phys.*, vol. 83, pp. 2742–2744, Mar. 1998.
- [8] N. A. Pertsev, A. G. Zembilgotov, and A. K. Tagantsev, "Effect of mechanical boundary conditions on phase diagrams of epitaxial ferroelectric thin films," *Phys. Rev. Lett.*, vol. 80, no. 9, pp. 1988–1991, 1998.
- [9] J. F. Scott, F. D. Morrison, M. Miyake, P. Zubko, X. J. Lou, V. M. Kugler, S. Rios, M. Zhang, T. Tatsuta, O. Tsuji, and T. J. Leedham, "Recent materials characterizations of [2D] and [3D] thin film ferroelectric structures," *J. Am. Ceram. Soc.*, vol. 88, no. 7, pp. 1691–1701, 2005.
- [10] S. S. N. Bharadwaja, D. J. Won, H. Fang, V. Gopalan, S. Trolier-McKinstry, N. Saldanha, and T. S. Mayer, "Processing and properties of high aspect ratio ferroelectric structures," in *Proc. 14th IEEE Int. Symp. Applications of Ferroelectrics*, 2004, pp. 189–192.
- [11] S. Bühlmann, B. Dwir, J. Baborowski, and P. Muralt, "Size effect in mesoscopic epitaxial ferroelectric structures: Increase of piezoelectric response with decreasing feature size," *Appl. Phys. Lett.*, vol. 80, pp. 3195–3197, Apr. 2002.
- [12] A. Stanishevsky, B. Nagaraj, J. Melngailis, R. Ramesh, L. Khriatchev, and E. McDaniel, "Radiation damage and its recovery in focused ion beam fabricated ferroelectric capacitors," *J. Appl. Phys.*, vol. 92, pp. 3275–3278, Sep. 2002.
- [13] G. Suyal, E. Colla, R. Gysel, M. Cantoni, and N. Setter, "Piezoelectric response and polarization switching in small anisotropic perovskite particles," *Nano Lett.*, vol. 4, no. 7, pp. 1339–1342, 2004.
- [14] I. Szafraniak, C. Harnagea, R. Scholz, S. Bhattacharyya, D. Hesse, and M. Alexe, "Ferroelectric epitaxial nano crystals obtained by a self-patterning method," *Appl. Phys. Lett.*, vol. 83, pp. 2211–2213, Sep. 2003.
- [15] S. Bühlmann, P. Muralt, and S. V. Allmen, "Lithography-modulated self-assembly of small ferroelectric  $\text{Pb}(\text{Zr},\text{Ti})\text{O}_3$  single crystals," *Appl. Phys. Lett.*, vol. 84, pp. 2614–2616, Apr. 2004.
- [16] S. S. N. Bharadwaja, M. Olszta, S. Trolier-McKinstry, X. Li, T. S. Mayer, and F. Roozeboom, "Fabrication of high aspect ratio ferroelectric microtubes by vacuum infiltration using macroporous silicon templates," *J. Am. Ceram. Soc.*, vol. 89, no. 9, pp. 2695–2701, 2006.
- [17] Y. Luo, I. Szafraniak, N. D. Zakharov, V. Nagarajan, M. Steinhart, R. B. Wehrspohn, J. H. Wendorff, R. Ramesh, and M. Alexe, "Nanoshell tubes of ferroelectric lead zirconate titanate and barium titanate," *Appl. Phys. Lett.*, vol. 83, pp. 440–442, Jul. 2003.
- [18] V. Nagarajan, A. Roytburd, A. Stanishevsky, S. Prasertchoung, T. Zhao, J. Melngailis, O. Auciello, and R. Ramesh, "Dynamics of ferroelastic domains in ferroelectric thin films," *Nat. Mater.*, vol. 2, no. 1, pp. 43–47, 2003.
- [19] W. Lee, H. Han, A. Lotnyk, M. A. Schubert, S. Senz, M. Alexe, D. Hesse, S. Baik, and U. Gösele, "Individually addressable epitaxial ferroelectric nanocapacitor arrays with near  $\text{Tb inch}^{-2}$  density," *Nat. Nanotechnol.*, vol. 3, no. 7, pp. 402–407, 2008.
- [20] A. Petraru, V. Nagarajan, H. Kohlstedt, R. Ramesh, D. G. Schlom, and R. Waser, "Simultaneous measurement of the piezoelectric and dielectric response of nanoscale ferroelectric capacitors by an atomic force microscopy based approach," *Appl. Phys. A*, vol. 84, no. 1–2, pp. 67–71, 2006.
- [21] M. Wegener and S. Bauer, "Micro storms in cellular polymers: A route to soft piezoelectric transducer materials with engineered macroscopic dipoles," *ChemPhysChem*, vol. 6, no. 6, pp. 1014–1025, 2005.
- [22] F. D. Morrison, L. Ramsay, and J. F. Scott, "High aspect ratio piezoelectric strontium–bismuth–tantalate nanotubes," *J. Phys. Condens. Matter*, vol. 15, no. 33, pp. L527–L531, 2003.
- [23] R. S. Rayleigh, "Notes on electricity and magnetism. III. On the behavior of iron and steel under the operation of feeble magnetic forces," *Philos. Mag.*, vol. 23, pp. 225–245, 1887.
- [24] D. Damjanovic, "Ferroelectric, dielectric and piezoelectric properties of ferroelectric thin films and ceramics," *Rep. Prog. Phys.*, vol. 61, no. 9, pp. 1267–1324, 1998.
- [25] P. Bettotti, L. Dal Negro, Z. Gaburro, L. Pavesi, A. Lui, M. Galli, M. Patrini, and F. Marabelli, "P-type macro porous silicon for two-dimensional photonic crystals," *J. Appl. Phys.*, vol. 92, pp. 6966–6972, Dec. 2002.
- [26] W. J. Paulus, M.S. thesis, Intercollege Program of Solid-State Science, The Pennsylvania State University, 1990.
- [27] J. F. Scott, "Ferroelectrics go bananas," *J. Phys. Condens. Matter*, vol. 20, no. 2, art. no. 021001, 2008.
- [28] M. Morge, E. T. Ryan, J.-H. Zhao, C. Hu, T. Cho, and P. S. Ho, "Low dielectric constant materials for ULSI interconnects," *Annu. Rev. Mater. Sci.*, vol. 30, pp. 645–680, Aug. 2000.
- [29] M. Tomar, V. Gupta, A. Mansingh, and K. Sreenivas, "Temperature stability of *c*-axis oriented  $\text{LiNbO}_3/\text{SiO}_2/\text{Si}$  thin film layered structures," *J. Phys. D Appl. Phys.*, vol. 34, no. 15, pp. 2267–2273, 2001.
- [30] Q. M. Zhang, W. Y. Pan, S. J. Jang, and L. E. Cross, "Domain wall excitations and their contributions to the weak-signal response of doped lead zirconate titanate ceramics," *J. Appl. Phys.*, vol. 64, pp. 6445–6451, Dec. 1988.
- [31] J. L. Jones, M. Hoffman, J. E. Daniels, and A. J. Studer, "Direct measurement of the domain switching contribution to the dynamic piezoelectric response in ferroelectric ceramics," *Appl. Phys. Lett.*, vol. 89, art. no. 092901, Aug. 2006.
- [32] O. Boser, "Statistical theory of hysteresis in ferroelectric materials," *J. Appl. Phys.*, vol. 62, pp. 1344–1348, Aug. 1987.
- [33] D. Damjanovic, "Stress and frequency dependence of the direct piezoelectric effect in ferroelectric ceramics," *J. Appl. Phys.*, vol. 82, pp. 1788–1797, Aug. 1997.
- [34] N. B. Gharb, I. Fujii, E. Hong, S. Trolier-McKinstry, D. V. Taylor, and D. Damjanovic, "Domain wall contributions to the properties of piezoelectric thin films," *J. Electroceram.*, vol. 19, no. 1, pp. 47–65, 2007.
- [35] D. Damjanovic, "Hysteresis in Piezoelectric and Ferroelectric Materials," in *The Science of Hysteresis*, vol. 3, G. Bertotti and I. Mayergoyz, Eds. Amsterdam, The Netherlands: Elsevier, 2005, ch. 4, pp. 337–465.
- [36] U. Robels and G. Arlt, "Domain wall clamping in ferroelectrics by orientation of defects," *J. Appl. Phys.*, vol. 73, pp. 3454–3460, Apr. 1993.
- [37] T. Nattermann, V. Pokrovsky, and V. M. Vinokur, "Hysteretic dynamics of domain walls at finite temperatures," *Phys. Rev. Lett.*, vol. 87, no. 19, art. no. 197005, 2001.
- [38] Q. M. Zhang, H. Wang, N. Kim, and L. E. Cross, "Direct evaluation of domain-wall and intrinsic contributions to the dielectric and piezoelectric response and their temperature dependence on lead-zirconate-titanate ceramics," *J. Appl. Phys.*, vol. 75, pp. 454–459, Jan. 1994.
- [39] G. Arlt, U. Böttger, and S. Witte, "Dielectric dispersion of ferroelectric ceramics and single crystals at microwave frequencies," *Ann. Phys.*, vol. 3, no. 7–8, pp. 578–588, 1994.
- [40] D. Damjanovic, EPFL, Switzerland, private communication, Mar. 2009.
- [41] C. A. Randall, N. Kim, J. P. Kucera, W. Cao, and T. R. Shrout, "Intrinsic and extrinsic size effects in fine-grained morphotropic-phase-boundary lead zirconate titanate ceramics," *J. Am. Ceram. Soc.*, vol. 81, no. 3, pp. 677–688, 1998.
- [42] R. Waser, "Dielectric analysis of integrated ceramic thin film capacitors," *Integr. Ferroelectr.*, vol. 15, no. 1, pp. 39–51, 1997.



**Srowthi S. N. Bharadwaja** received the B.S. degree in mathematics, physics and chemistry in 1994, an M.S. in solid state physics in 1996 from Nagarjuna University, India, and a Ph.D. degree in materials science and engineering from the Indian Institute of Sciences, Bangalore, India, in 2002. His Ph.D. research revolved around antiferroelectric thin films for charge storage and MEMS device applications. He worked (2001–2003) in Laboratoire de Ceramique as a postdoctoral scholar at the École Polytechnique Federale de Lausanne, Switzerland. In 2003, he moved to The Pennsylvania State University as a postdoctoral scholar and became a Research Associate in 2005 at the Materials Research Institute. His research interests include

bulk and thin films of ferroelectric materials, electronic thin films processing via physical and chemical deposition methods, and electrical, thermal, magnetic and piezoelectric characterization of thin films for various MEMS device applications. To date, he has published approximately 48 papers in peer reviewed journals. Currently he is developing laser assisted low temperature ( $< 350$  °C) crystallization process for electroceramic thin film for MEMS applications and is working on bolometer thin films for night vision applications. He is a member of Materials Research Society and the IEEE Ultrasonics, Ferroelectrics, and Frequency Control Society.



**Paul J. Moses** received the B.A. degree in mathematics and physics and the M.A. degree in mathematics in 1987 and 1989, respectively, from The Pennsylvania State University. He is a Senior Research Assistant at the Materials Research Institute, The Pennsylvania State University. Before his current position, he worked as a Research Engineer and a Research Consultant in many academic institutes. His research interests include designing A/D electronic testing setups, DC and RF electromagnetic setups, computer system programming and interfacing, and electrical equipment setups for dielectric and piezoelectric measurements. For this work, he developed a low-noise lock-in amplifier-based ultra small ferroelectric capacitance measurement ( $< 10^{-15}$  F) setup to characterize ferroelectric microtube structures. So far, he has authored or co-authored approximately 25 publications in various international journals and conference proceedings.



**Susan Troler-McKinstry** received the B.S., M.S., and Ph.D. degrees in ceramic science from The Pennsylvania State University, University Park. She is currently a Professor of Ceramic Science and Engineering and Director of the W. M. Keck Smart Materials Integration Laboratory, The Pennsylvania State University. She has held visiting appointments with the Hitachi Central Research Laboratory, the U.S. Army Research Laboratory, and the Ecole Polytechnique Federale de Lausanne. Her main research interests include dielectric and piezoelectric thin films, the development of texture in bulk ceramic piezoelectrics, and spectroscopic ellipsometry. She is a fellow of the American Ceramic Society, an academician of the World Academy of Ceramics, a fellow of IEEE, and a member of the Materials Research Society. She is past-president of both the Keramos and the Ceramics Education Council. She is co-chair of the committee revising the *IEEE Standard on Ferroelectricity*. She is currently the junior past president of the IEEE Ultrasonics, Ferroelectrics, and Frequency Control (UFFC) Society.



**Theresa S. Mayer** received the B.S. degree in electrical engineering from Virginia Tech in 1988, and the M.S. and Ph.D. degrees in electrical engineering from Purdue University in 1989 and 1993, respectively. In 1994, she joined the Department of Electrical Engineering at Penn State University-University Park, where she is a Professor. Dr. Mayer was appointed as an Associate Director of the Penn State University Materials Research Institute in 2006, where she serves as the Technical

Director of Penn State Nanofabrication Facility. She is also the Director of the Penn State Site of the National Science Foundation National Nanotechnology Infrastructure Network (NSF-NNIN). Her interests are in the areas of nanoscale electronic and optical device fabrication, integration, and characterization. Her group currently has funded projects in semiconductor nanowire electronics, self-assembly of chemical and biological sensors on CMOS chips, metallo- and all-dielectric metamaterials, and molecular electronic devices. Prof. Mayer was a Kodak Fellow (1990 to 1993) and the recipient of a National Science Foundation CAREER Award (1995) and a Penn State Engineering Society Outstanding Teaching Award (2000). She served as the General Chair of the IEEE Device Research Conference and the Chair of the Gordon Research Conference on the Chemistry and Physics of Nanostructure Fabrication in 2006. Dr. Mayer holds 5 U.S. patents and is the co-author of over 100 journal publications.



**Paolo Bettotti** was born on June 18, 1976 in Italy. He is currently working as a post-doctoral fellow at the Department of Physics of the University of Trento. He earned his M.S. degree from University of Padua in 2000, *summa cum laude*, and his Ph.D. degree at the University of Trento in 2004. His current research interests are silicon based nanophotonics and in nanophotonic systems composed by hybrid materials for sensing applications. His main expertise spans over structural and spectroscopical characterization (AFM and

SNOM, SEM, optical spectroscopy, spectroscopy of gaining media) of materials and modeling of complex photonic structures (1-D and 2-D photonic crystals, slot waveguides, and coupled resonator systems). He has published more than 20 articles so far as an author or co-author in peer reviewed journals.



**Lorenzo Pavesi** was born on November 21, 1961. He received his Ph.D. in physics at the Ecole Polytechnique Federale de Lausanne (Switzerland) in year 1990. Currently, he is a Full Professor at the University of Trento. He founded the research activity in semiconductor optoelectronics at the University of Trento and leads the nanoscience laboratory. His research activity concerned silicon-based photonics where he looks for the convergence between photonics and electronics by using silicon nanostructures. He is interested in active

photonics devices which can be integrated in silicon by using classical waveguides or novel waveguides such as those based on dynamical photonic crystals. His interests encompass also optical sensors or biosensors and solar cells. He is an author and co-author of more than 250 papers, author of several reviews, editor of more than 10 books, author of 2 books, and holds six patents. He holds an H-number of 35 according to the Web of Science.